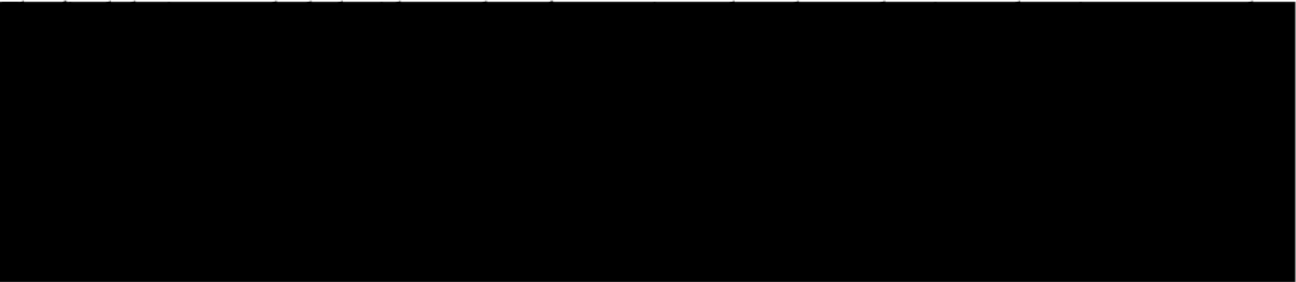


Airbus Sloshing Rocket Workshop 2024

Abstract

Exploring the dynamics of sloshing liquids in the aerospace sector is essential for enhancing performance, safety, and structural integrity, thereby supporting sustainable practices within the industry. The Airbus Sloshing Rocket Workshop challenges students to simulate real-world aerospace conditions to explore the implications of sloshing. This paper investigates the optimal design of a low-cost reusable water rocket made by the team [REDACTED]. This system incorporates a vector and a passive stabilisation system to control the movement of water stored in an additional unpressurised tank. To achieve this, findings of a literature study were used to develop two concept designs: a glide focused and a rocket focused. The former was selected and designed in greater detail.

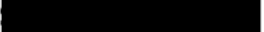


Contents

Abstract	ii
List of Figures	v
List of Tables	vi
Nomenclature	vii
1 Introduction	1
2 Literature Study	2
2.1 Sloshing Phenomenon	2
2.2 Innovative sloshing mitigation ideas	3
2.2.1 Active control	3
2.2.2 Passive control	3
3 Requirements Capture	5
3.1 Competition's Scoring Formula	5
3.2 List of Requirements	5
4 Concept Design	8
4.1 Passive Versus Active Means of Control	8
4.2 Concept Number 1: Rocket focused	8
4.3 Concept Number 2: Glider focused	11
4.4 Concept Design Decision	13
4.4.1 Preliminary Aerodynamic Design	14
4.4.2 Preliminary Rocket Design	14
4.4.3 Preliminary Sloshing Tank Design	15
5 Detailed Design	18
5.1 Final Configuration	18
5.2 Propellant mass estimation	19
5.3 Pressure vessel design	20
5.4 Wing design	20
5.5 Rear tail	21
5.5.1 Horizontal tail	21
5.5.2 Vertical tail	22
5.5.3 V-tail sizing	22
5.6 Sloshing Tank	22
5.6.1 Tank Design	22
5.6.2 Tank positioning	23
5.7 Nosecone	24
5.8 Launch Mechanism	24
5.9 CAD model	25
5.10 Manufacturing Process	27
5.10.1 Bill of Materials	27
5.10.2 Manufacturing Plan	28

6	Design Verification and Validation	32
6.1	Simulation Tools Used	32
6.2	Requirements' Assessment	34
7	Conclusion	37
A	Coding and Simulations	41

List of Figures

2.1	Tank Sloshing	2
2.2	Modelling of sloshing	3
4.1	Rocket-focused Free-Body Diagram	9
4.2	Three possible designs	11
4.3	Trigonometric Relation between flight angle, distance covered and flight height parameters	11
4.4	Aerodynamic Relations between Forces and Kinematic parameters	12
4.5	Preliminary CAD model of the Glider Concept	13
4.6	The three axes of aircraft stability (n.d.)	15
4.7	Pitching Moment as a result of a positive angle of attack disturbance Hoekstra, 2023 .	16
5.1	Preliminary Doodle to assist in the visualization of the team's ideation	19
5.2	Preliminary pressure vessel render	20
5.3	Airfoil 	21
5.4	Preliminary sloshing tank render	23
5.5	Render of nosecone	24
5.6	Preliminary Doodle of the Launching Pad	24
5.7	Presentation of CAD model	25
6.1	The estimated trajectory of a balanced gliding rocket	32
6.2	The estimated trajectory of a balanced gliding rocket	33
6.3	Input and output values for the online simulation tool Jackiewicz, n.d.	34
7.1	Repeated Presentation of CAD model	37

List of Tables

3.1	Functional Requirements	6
3.2	Performance Requirements	6
3.3	Design Requirements	7
3.4	Operational Requirements	7
5.1	Design values for the pressure vessel	20
5.2	Design values for the wing	21
5.3	Design values for the horizontal tail	21
5.4	Design values for the horizontal tail	22
5.5	Design values for the vertical tail	22
5.6	Advantages and Disadvantages of two sloshing tank placement options	23
5.7	Bill of Materials	28
6.1	Assessment of Functional Requirements	35
6.2	Assessment of Performance Requirements	35
6.3	Assessment of Design Requirements	35
6.4	Assessment of Operational Requirements	36

Nomenclature

Abbreviations

Abbreviation	Definition
ISA	International Standard Atmosphere
MTOW	Maximum Take-Off Weight

Symbols

Symbol	Definition	Unit
A	Cross-sectional area	[m ²]
a	Acceleration	[m/s ²]
b	Span	[m]
c	chord	[m]
CG	Center of Gravity	[m]
C_d	Drag coefficient	[-]
C_L	Lift Coefficient	[-]
C_m0	Total moment	[Nm]
$C_m a$	Moment about aerodynamic center	[Nm]
D	Drag force	[N]
F_{net}	Net Force	[N]
g	Gravitational acceleration	[m/s ²]
h	Height	[m]
L	Lift Force	[N]
S	Wing Area	[N]
t	Time	[s]
T	Thrust	[N]
V	Velocity	[m/s]
V_0	Initial Velocity	[m/s]
V_h	Volume coefficient	[-]
V_t	Terminal Velocity	[m/s]
W	Weight	[N]
x	Horizontal Position	[m]
y	Vertical position	[m]
α	Angle of attack	[deg]
ρ	Density	[kg/m ³]
γ	Descent angle	[deg]
ϕ	Dihedral angle	[deg]

Introduction

Understanding the dynamics of sloshing liquids within the aerospace industry plays a vital role in ensuring optimal performance, safety, and structural integrity of the design. In aviation, sloshing mitigation promotes sustainable practices in a world where the extensive consequences of climate change are becoming evident (Colville, 2024). The challenge of sloshing extends to spacecraft, where sloshing in microgravity poses unique challenges due to the lack of a consistent gravitational force to dampen liquid movements (Simonini et al., 2024). Consequently, ongoing research is being done towards the development of sloshing mitigation strategies for both aircraft and spacecraft. These efforts aim to reduce the sloshing phenomenon within the fuel systems, thereby increasing efficient operations and overall stability.

The report's objective is the description of the design approach of a low-cost reusable water rocket incorporating a vector and passive stabilisation system to control the movement of water stored in an additional unpressurised tank. Specifically, the design should include one unpressurised tank containing a minimum of 500ml of water with a fill level of 50% and 1 or more pressurised tanks containing water for propulsion. The primary goal of this rocket is to optimise its flight performance in terms of distance covered, total flight time as well as maximising payload mass while keeping take-off mass low. The methodology employed to ensure that all requirements are satisfied consisted of several steps, including clearly establishing the objectives and constraints of the design, stating assumptions made along the way, developing concept designs, and choosing a design concept. Decisions were validated by coding scripts and simulation tools along the design process.

The report will be presented in the following structure. chapter 2 will provide a theoretical background on the challenge of sloshing liquid propellants in the aerospace industry and delve into innovative ideas used for sloshing minimisation. chapter 4 will explore possible designs and chapter 5 will explain in detail the selected design together with a manufacturing plan. Moreover, chapter 6 will demonstrate how the final design meets all the requirements and validate the techniques used along the process. Along with the submission of the report a risk assessment will be provided identifying the possible hazards and mitigation strategies.

Lastly, effective team organisation is the cornerstone of a successful project. A Gantt Chart was created to document the progress of the design and responsibilities were split depending on the availability of each team member. This was crucial in order to balance the completion of this project along with our current career pursuits and demanding academic schedule. In short, multiple brainstorming sessions were done during the concept design phase and a concurrent engineering approach was adopted for the detailed design phase.

2

Literature Study

Just like in every engineering project, a literature study is performed to provide the necessary understanding, knowledge and assets to progress the design. This literature review is centered around two levels: first, the sloshing phenomenon. This includes understanding of the phenomenon, empirical formulas and equations. Then developments in the topic of sloshing mitigation are explored, with an emphasis on concepts viable for integration into this competition's framework.

2.1. Sloshing Phenomenon

Sloshing is a phenomenon that occurs in fluids and can be defined as the fluid's dynamic response to disturbances (Ibrahim, 2005), as presented visually in Figure 2.1. The various sloshing modes or regimes, depend on the force field that acts on the fluid within the tank. The principal regimes can be split down into three: Constant force field, where a constant field like a gravitational field or a magnetic field act on the fluid, a zero acceleration case and an accelerated motion case. For this particular water rocket design, all three phases are experienced: accelerated motion takes place during ascent, zero acceleration at the transition phase and finally, a constant force field at the gliding phase.

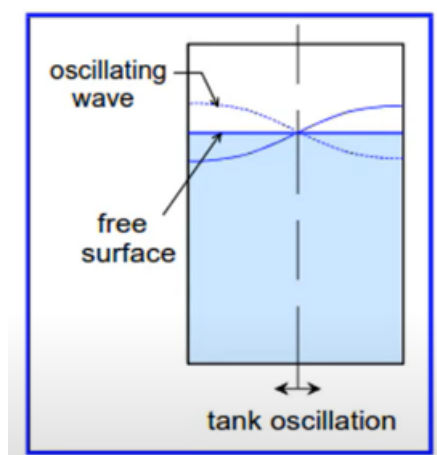


Figure 2.1: Tank Sloshing

Like most fluid phenomena, sloshing is not easily modelled analytically; the movement of the fluid depends on the initial boundary conditions, varying parameters such as viscosity and temperature, and the forces applied. To simplify the complexity of small amplitude sloshing, linear models are commonly used associated with the degrees of freedom, namely, the mass-spring-damper model and the pendulum model [2]. These two models are portrayed in Figure 2.2 Though, the motion of the

complete system is not considered in this analysis limiting its applicability [2].

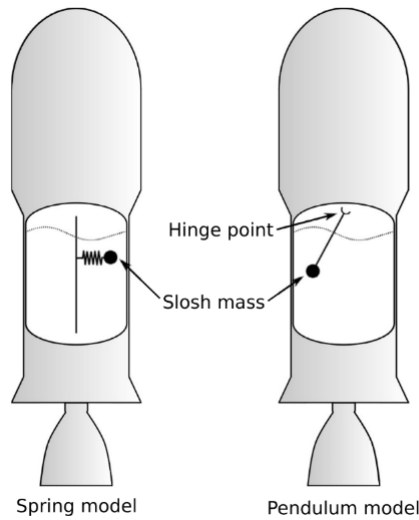


Figure 2.2: Modelling of sloshing

2.2. Innovative sloshing mitigation ideas

Multiple active and passive control ideas have been developed to minimize this effect not only in the aerospace sector but in various industries including maritime and automotive.

2.2.1. Active control

Active control is driven using simulations tools to predict the realistic motion of the fluid and the shift of the center of gravity. When forces act on a rigid body, the fluids in the tank experience acceleration and thus displacement which can be approximated with advanced high-fidelity CFD tools (Behruzi and Rose, 2018, Simonini et al., 2024). The process is as follows: a controller receives the velocity and position of the object in the form of a state vector, performing an evaluation of the current state and initiating a correction if the displacement exceeds its maximum value (Behruzi and Rose, 2018). To this day, sloshing modelling remains a rather challenging task especially combined with strict deadlines and as a result it is rarely used in simple aerospace applications (Simonini et al., 2024).

2.2.2. Passive control

Passive control entails implementing features within the tank to minimize sloshing without requiring active control mechanical systems and are frequently used in various applications.

Pressure distribution of the sloshing fluid varies depending on the **tank geometry**. Taking into consideration the simplest case, a rectangular tank, it was found that adding chamfers can reduce the sloshing of the fluid due to lower pressure distribution measurements and different wave shapes at the same natural frequency ratios (Korkmaz, 2022). Additionally, longer tanks tend to have reduced instantaneous wave amplitudes, while deeper liquid levels lead to stronger sloshing effects characterized by larger waves (Hosseini and Farshadmanesh, 2011). In a more detailed study conducted by S. Utami et. al., a variation of tank shapes was investigated which included a prismatic, a rectangle, a tube, a spherical and finally a combination of a spherical and tube model referred to as “new model” (Utami et al., 2023). The study was conducted using Smoothed Particle Hydrodynamics (SPH), a Lagrangian, mesh-free method along with Blender for advanced visualization of fluid dynamics (Utami et al., 2023). The findings suggested that tube tanks are optimal among the conventional shapes for tank geometry, but the new model demonstrated significant potential (Utami et al., 2023).

Baffles are commonly used to limit the flow of the liquid and dissipate energy. Taking the simplest

case of rigid baffles, it was found that a vertical centered baffle is optimal for its simplicity and good performance for minimizing the horizontal harmonic excitations (Peromingo et al., 2023). Placing two or three vertical baffles evenly spaced throughout the length of the tank can further reduce the sloshing effect, while additional baffles have a minimal impact (Hosseini and Farshadmanesh, 2011). Furthermore, there exists an optimal baffle submersion depth; submerging a baffle deeper does not affect the maximum water level variations and thus can be removed ensuring a lower overall weight (Hosseini and Farshadmanesh, 2011). Analogously, horizontal baffles are used to control the sloshing along the vertical axis of the tank and other rotational movements (Hosseini and Farshadmanesh, 2011). A microscopic model and a volume-averaged macroscopic model investigation showed that side-mounted placement is also effective, but the exact positioning requires accurate predictions of the fluid movement (Wang et al., 2023).

For weight saving purposes, a **flexible baffle** proved to be increasingly effective compared to a rigid baffle of the same width, with the implication that the “damping factor was at least as great as that of a rigid baffle of the same width” (Dodge, 1971). Nonetheless, the idea of **flexible tank walls** can be disregarded as it amplified the amplitude of the sloshing and extended the response period highlighting the sloshing dynamics (Khouf et al., 2023).

Today, more advanced baffles designs have been designed and researched. For instance, the presence of **porous media** placed inside the tank can substantially influence the dynamic characteristics of the sloshing behavior particularly in the first sloshing mode by providing a damping effect to the liquid (Tsao and Huang, 2021). Moreover, numerical models derived that submerged passive **moving baffles** implementing linear springs can reduce the kinetic energy of the fluid up to 23% (Gligor et al., 2024).

Another innovative idea for sloshing reduction is the use of **floating balls and surfaces** along the free surface of the liquid inside the tank (Gurusamy, 2023). A comprehensive study by S. Gurusamy proved that “three-dimensional nonlinear sloshing states” were mitigated using floating balls. Moreover, an experimental analysis justified the use of floating balls was particularly effective in shallow to intermediate water depths and higher sloshing modes (Gurusamy, 2023). Similarly, it has been discovered that, in comparison to a clean tank, the presence of two perforated floating plates within the tank can significantly reduce the occurrence of strong resonant sloshing responses, particularly when the external excitation frequency is close to the first-order resonant frequency (Dodge, 1971).

3

Requirements Capture

Understanding the requirements is fundamental in engineering practise. Engineering entails optimising the design within the given limitations, requirements, resources and time frames. Adhering to the requirements ensures that the final product meets the specified needs and expectations of the organisers, including safety, functionality, and regulatory standards. Moreover, it minimizes the risk of failure and costly rework, while enhancing reliability and performance. This section enumerates the requirements imposed by the organisers providing the team and the users constant access and guidance.

3.1. Competition's Scoring Formula

Before presenting the requirements, it is very important to highlight the purpose of the design, using the competition's predicted flight score formula:

$$\text{SCORE} = (\text{Time}[s] + \text{Distance}[m]) \times \frac{\text{Payload [Kg]}}{\text{MTOW[Kg]}} \quad (3.1)$$

This formula acts as a design criterion in the design phase limiting the viable options and arriving to possible design concepts.

3.2. List of Requirements

The requirements were split into four categories, namely, functionality, performance, design and operation. Along with every requirement, a rationale was provided together with the source. The requirements of each category are listed in Table 3.1, Table 3.2, Table 3.3 and Table 3.4 respectively.

ID	Requirement	Rationale	Source

Table 3.1: Functional Requirements

ID	Requirement	Rationale	Source

Table 3.2: Performance Requirements

ID	Requirement	Rationale	Source

Table 3.3: Design Requirements

ID	Requirement	Rationale	Source

Table 3.4: Operational Requirements

4

Concept Design

Concept design is a critical phase in rocket development, especially for addressing the complex challenge of sloshing. A robust concept design lays the foundation for the detailed design that follows, while ensuring that the designs meets all specified requirements, found in chapter 3. This section involves deciding between active and passive control and analyses two design alternatives, each with a different design philosophy. The first concept optimises the rocket aspect, placing bottles in parallel to maximise the apogee, with the secondary goal of maximising airborne time, and endurance. The second concept is a long, multiple-bottles in series design that focuses on aerodynamic gliding performance.

4.1. Passive Versus Active Means of Control

One of the key design decisions is whether to use passive or active control systems. Passive control systems are simple, reliable, and cost-effective, making them suitable for tight project constraints. Unlike active systems, which need complex sensors, actuators, and control algorithms, passive solutions rely on mechanical design and aerodynamic principles for stability and control.

Given the competition requirements, our limited experience with control theory, and time constraints, we chose passive control methods. Airfoil shaping, wing dihedral, and aerodynamic surfaces are examples of passive mechanisms that reduce development time, cost, and potential failure points.

4.2. Concept Number 1: Rocket focused

The first concept, focuses on the design of an efficient water rocket, sacrificing some of the glider performance but aiming to increase the time spent airborne. This is going to be done by attempting to minimize drag and weight and maximizing the thrust, propelling the rocket as high as possible. With the vehicle essentially becoming a projectile, simple projectile motion can be used to estimate the trajectory of the rocket, with the goal of maximizing its apogee.

Mechanics Analysis

In order to identify the optimization criteria for this design, an analysis of the forces that act on it throughout the flight is necessary. Starting with mechanics, the following diagram can be drawn:

Naturally, it can be deduced that the thrust has to be as large as possible, in order to exceed the aerodynamic drag and the weight of the rocket. Therefore, as mentioned before, both drag and weight have to be minimized. Starting with drag, which is equal to:

$$D = C_d \cdot \frac{1}{2} \cdot v^2 \cdot A \cdot \rho$$



Figure 4.1: Rocket-focused Free-Body Diagram

We assume the altitude change is small enough to keep the density constant. Therefore, the only changing parameter is velocity, and the adjustable parameters are the drag coefficient and the cross-sectional area A . Minimizing the cross-sectional area suggests using a long, slender bottle, while minimizing the drag coefficient requires an aerodynamically efficient design.

$$F_{net} = -W - D \quad (4.1)$$

Dividing Equation 4.1 by the mass, and expanding the drag force term, the net acceleration of the rocket during ascent is obtained:

$$a_{net} = -g - \frac{C_d \cdot v^2 \cdot \rho \cdot A}{2m}$$

As acceleration can be written as the change in velocity over the change in time and, if the right hand side of the above mentioned equation is multiplied by $\frac{g}{g}$ and using the definition of terminal velocity, V_t the following can be obtained:

$$a = \frac{dv}{dt} = -g \cdot \frac{1 + v^2}{V_t^2} \quad (4.2)$$

$$\begin{aligned} \frac{V_t^2}{1 + v^2} dv &= -g dt \\ \arctan\left(\frac{V}{V_t}\right) - \arctan\left(\frac{V_0}{V_t}\right) &= \frac{-g \cdot t}{V_t} \end{aligned}$$

Taking tangent of both sides and using the trigonometric identity for the tangent $\tan(a - b)$, the following relation can be obtained:

$$\frac{V}{V_t} = \frac{\frac{V_0}{V_t} - \tan\left(\frac{g \cdot t}{V_t}\right)}{1 + \frac{V_0}{V_t} \cdot \tan\left(\frac{g \cdot t}{V_t}\right)} \quad (4.3)$$

By setting V equal to zero in Equation 4.3, one can compute the time when the apogee is reached. Coming back to the first line of Equation 4.2, one can rearrange to obtain a different differential equation:

$$\begin{aligned} a &= \frac{dv}{dt} = \frac{dv}{dy} \cdot \frac{dy}{dt} = v \cdot \frac{dv}{dy} \\ v \cdot \frac{dv}{dy} &= -g \cdot \frac{1 + v^2}{V_t^2} \\ \frac{V_t^2 \cdot v}{1 + v^2} dv &= -g dy \end{aligned}$$

Once again, integrating and rearranging one can obtain the following equation which describes the height of the rocket as a function of velocity, V .

$$y = \frac{V_t^2}{2g} \cdot \ln\left(\frac{V_0^2 + V_t^2}{V^2 + V_t^2}\right) \quad (4.4)$$

Finally, setting V equal to 0, Equation 4.4 becomes:

$$y_{max} = \frac{V_t^2}{2g} \cdot \ln\left(\frac{V_0^2 + V_t^2}{V_t^2}\right) \quad (4.5)$$

As can be deduced from the above, maximization of terminal velocity as well as burn-out velocity will result in the maximization of the height. Coming back to Equation 4.3, a similar conclusion can be drawn to maximize the time, t :

$$t_{max} = \frac{V_t}{g} \cdot \arctan\left(\frac{V_0}{V_t}\right) \quad (4.6)$$

Once again, increasing both velocities should result in a large ascent time, maximizing the team's score.

Having a look at the descent phase, once again the only two forces acting on the rocket are its weight and its drag. Terminal velocity is reached when the two are equal. The motion can be split up into two phases: the acceleration phase, where the rocket accelerates from 0 vertical velocity to its terminal velocity and the constant speed phase, where the rocket maintains a constant vertical velocity. For this stage of the design however, the following equation can be used as a good approximation of the time it takes to reach the ground (Mushtaq, 2023):

$$t = \sqrt{\frac{2 \cdot h}{g}} \quad (4.7)$$

Finally, the total airborne time, which is what this design aims for, is equal to the sum of Equation 4.7 and Equation 4.6. To get a better general idea of the design that could be used, three renders of rocket designs are shown below, where the blue part represents the bottles or the thrust section of the rocket, the purple is the location of the sloshing tank and the grey part is the protective shroud:

(a) High slenderness ratio rocket

(b) Standard 2-liter bottle rocket.

(c) Maximum Thrust Design with three bottles

Figure 4.2: Three possible designs

4.3. Concept Number 2: Glider focused

The second concept mainly focuses on designing an optimized glider, and thus sacrificing a bit of the rocket capabilities of the model. This decision aligns with the grading formula in chapter 3, where the "Flight Time" and the "Distance Covered" carry significant weight, aspects that gliders excel at (Voskuijl, 2024). Thus this concept focuses on minimising the descent angle on a constant speed, finding the perfect balance between endurance and range.

Flight Mechanics Analysis

The following flight mechanics analysis includes a lot of assumptions that diverge from the actual flight conditions. It was deemed crucial to start from this foundation as initial assumptions provide a solid framework for subsequent enhancements and refinements, providing invaluable insights on the conceptualization and development of the glider model. Specifically, it is assumed that the glider is flying in steady, level flight. Additionally, the lift-to-drag ratio ($\frac{C_L}{C_D}$) is considered constant. This is a valid assumption as the aerodynamic coefficients depend on the airfoil shape and geometry, angle of attack, velocity and aspect ratio, all of which are expected to be constant at the gliding phase of the flight (Voskuijl, 2024).

Trigonometric Relation

To derive the relation between the flight path angle (γ) and the distances in question, we start with the basic equations of aerodynamics and flight mechanics (Voskuijl, 2024). Consider the glider shown in Figure 4.4:

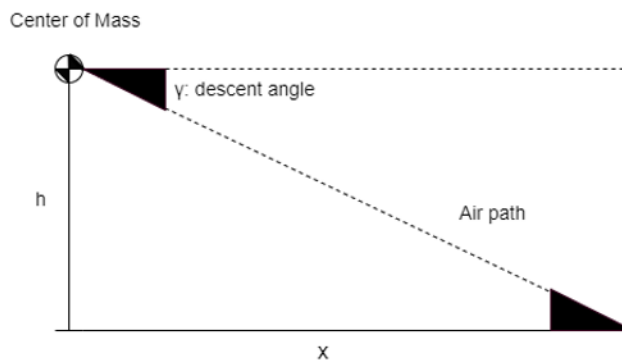


Figure 4.3: Trigonometric Relation between flight angle, distance covered and flight height parameters

At this figure the centre of mass of the glider is depicted, the descent angle γ , the flight height (h) and the distance covered (x). With simple trigonometry it is evident that these parameters are related through Equation 4.8.

$$\gamma = \arctan\left(\frac{h}{x}\right) \quad (4.8)$$

This is the trigonometric relation of γ , relating the angle with the distance parameters (Voskuijl, 2024).

Aerodynamic Relation

The flight performance relationships are then derived based on the following figure:

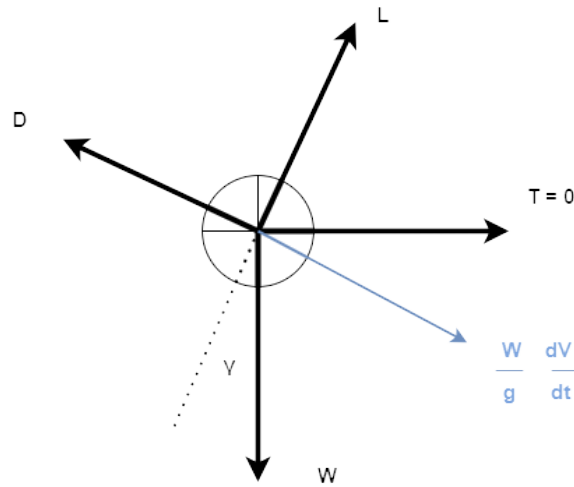


Figure 4.4: Aerodynamic Relations between Forces and Kinematic parameters

The vectors in grey are the forces that act on the glider, and the blue are the kinematic relations namely the mass times the acceleration. Notice that the thrust is equal to zero as the glider has no propulsion system. Additionally, the descent angle should be small to maximize flight distance, and thus the small angle approximation can be used (Voskuijl, 2024):

$$\sin \gamma = 0 \quad (4.9)$$

$$\cos \gamma = 1 \quad (4.10)$$

Now the following relations can be derived:

$$-D - W \cdot \sin \gamma = 0 \quad (4.11)$$

$$L - W \cdot \cos \gamma = 0 \quad (4.12)$$

Applying the small angle approximations:

$$\gamma = \arcsin \frac{D}{W} \quad (4.13)$$

$$L = W \quad (4.14)$$

Now using the following standard aerodynamic equations:

$$1. \text{ Lift Equation: } L = \frac{1}{2} \rho V^2 S C_L$$

$$2. \text{ Drag Equation: } D = \frac{1}{2} \rho V^2 S C_D$$

As derived above in steady, level flight, the lift force must balance the weight of the glider:

$$L = W$$

Substituting the expressions for lift and drag from the lift and drag equations:

$$\frac{1}{2} \rho V^2 S C_L = \frac{1}{2} \rho V^2 S C_D$$

Now, we can rearrange this equation to find the relationship between C_L and C_D :

$$\frac{C_L}{C_D} = \frac{L}{D} = \frac{W}{D}$$

And as a result,

$$\gamma_{min} = \arcsin \frac{1}{\frac{C_L}{C_{D_{max}}}} \quad (4.15)$$

In conclusion, in steady, level flight, the flight path angle (γ) is related to the lift-to-drag ratio ($\frac{C_L}{C_D}$) through trigonometric relationships. In the previous section, $\gamma = \arcsin\left(\frac{C_L}{C_D}\right)$ and $\gamma = \arctan\left(\frac{h}{x}\right)$ were derived. Considering that, the flight height is primarily defined by the rocket characteristics, it will be considered constant at this point. Thus from Equation 4.8 we can easily derive that to maximize the flight distance x , we need to minimize the flight path angle γ ! Consequently, from Equation 4.15, in order to minimize the angle we need to maximize the lift-to-drag ratio ($\frac{C_L}{C_D}$)(Voskuijl, 2024).

As a final note, notice that endurance also depends on the flight angle and in fact is maximized when the the lift-to-drag ratio ($\frac{C_L}{C_D}$) is maximized as well (Voskuijl, 2024). So by twisting and optimising the aerodynamic parameters we can easily achieve the desired results for both maximum range and endurance!

A preliminary CAD version of Concept number one can be seen below:

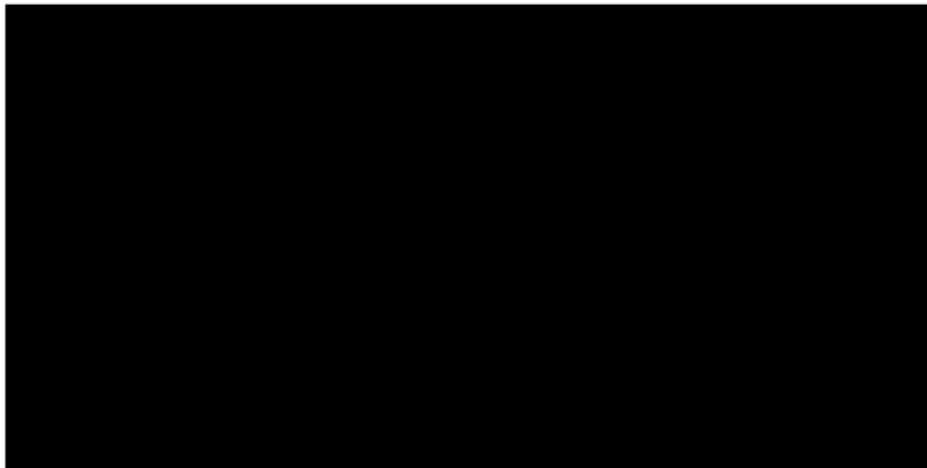


Figure 4.5: Preliminary CAD model of the Glider Concept

4.4. Concept Design Decision

Having discussed the above and studying the scoring formula in more detail, the team decided to maximize gliding performance while sacrificing a bit of rocket performance, as seen in the code of chapter 6.

4.4.1. Preliminary Aerodynamic Design

In order to maximise the lift while minimizing the drag, the following decisions were made based on the team's efforts to enhance passive aerodynamic control (Voskuijl, 2024):

- | | |
|---------------------------------------|---|
| 1. Airfoil Selection: | High-lift, low-drag airfoil optimized for low-speed flight and angles of attack. (Anderson, 2011) |
| 2. High Aspect Ratio: | Optimize for a high aspect ratio wing to maximize lift while minimizing induced drag. |
| 3. Dihedral for Stability: | Incorporate dihedral angle in the wing design to provide inherent stability and improve roll response. |
| 4. Lightweight Construction: | Use lightweight materials to minimize structural weight. |
| 5. Minimalist Fuselage Design: | Design a streamlined fuselage with minimal frontal area to reduce parasitic drag. |
| 6. V-tail Configuration: | Implement a V-tail configuration for the empennage to reduce drag and enhance directional stability.(Anderson, 2011 |

For the airfoil selection, the team opted for the [REDACTED] Airfoils which are commonly used in gliders. Regarding the use of lightweight Materials, while increasing weight is known for maximizing distance while minimizing endurance,minimising weight is considered for rocket characteristic reasons rather than purely aerodynamic ones, optimising its dual purpose. The decision to incorporate a dihedral and v-tail, stems from the belief that passive means of control are the most appropriate as described in section 4.1. Dihedral provides lateral stability,reducing unfavorable yaw tendencies (Voskuijl, 2024), while the V-tail combines pitch and yaw control into a single surface, lowering parasitic drag and improving overall performance (Voskuijl, 2024).

4.4.2. Preliminary Rocket Design

This concept prioritizes the aircraft over the spacecraft aspect of the competition. Nonetheless, achieving sufficient launch height is crucial for gliding performance, as shown in Equation 4.8.

The goal is to create a controlled asymmetry to deviate the rocket from a vertical path, transitioning smoothly to a gliding descent. The hybrid rocket-glider design incorporates features for powered ascent and unpowered descent, ensuring a smooth transition from the rocket stage to the aircraft phase.

Nozzle

A 3D-printed nozzle was considered, but due to concerns about on-site construction time and material availability, a simpler, effective nozzle was chosen.

A garden hose quick-release connector serves as the launch mechanism. By attaching a launch cord to a base and screwing the female part into it, the connection clasp opens, creating a launcher. The rocket will be launched at [REDACTED]e, providing the desired tilt.

Fins

Fin design is crucial for creating controlled asymmetry for the rocket-to-glider transition. The fins should be placed as far back on the rocket as possible to maximize stabilizing force by increasing the momentum per unit area from the aerodynamic center. This allows for smaller fins to use, to reduce drag and improve performance. Trapezoidal fins are chosen for their balance between the advantages of rectangular and swept fins, being cost-effective and easy to manufacture (Sutton and Biblarz, 2017).

Fuselage

The fuselage is primarily designed with the purpose of minimising parasitic drag. Thus a long multi-bottle one was chosen, where the bottles are placed in series, reducing the surface area, and minimizing complexity as no dispatch mechanics and complex connections are necessary. Additionally, it ensures uniform aerodynamic properties along its length, reducing insecurities and instabilities and enhancing accuracy.

4.4.3. Preliminary Sloshing Tank Design

The tank design is essential for dealing with sloshing. The concept selection is based on the literature review (chapter 2). Concepts were ruled out and selections were made and further optimisation takes place in the detailed design accounting for the materials constraints. Having that said, this concept favours simplicity, lightweightness and passive means of control and is performed in two levels. Firstly, the design of the actual tank to mitigate sloshing, and secondly the positioning of the tank to maintain stability and pitch control. As a result the following design is proposed:

Configuration of Slosh-Resistant Tank:

1. **Internal Baffles:** Baffles will be strategically placed within the tank to disrupt fluid motion and dampen sloshing. These baffles aim to dissipate the kinetic energy stored in the fluid area, while also partition the liquid stored which is vital in controlling the sloshing phenomenon.
2. **Hourglass Tank Shape:** The hourglass tank shape will minimise the surface area during ascent and the fluid motion during the gliding phase.
3. **Internal Net with floating balls:** An internal net will be installed with fixed floating balls to dissipate the liquid's kinetic energy, reduce sloshing, and minimize the risk of dynamic loads on the tank structure.

The exact design, which concerns dimensioning, placement and amount, will be finalised at the detailed design where the configuration optimised. Focus will be placed on avoiding "over-engineering" the tank and making it too heavy.

Positioning

Placing the tank, i.e. the payload of our model is extremely important for stability. There are three axes of control that this analysis is concerned about. These can be seen at Figure 4.6:

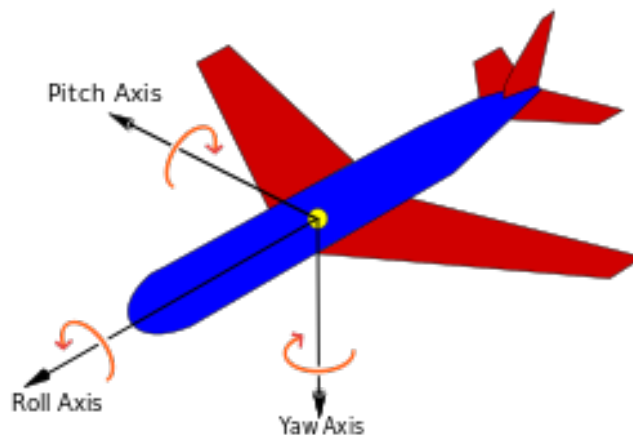


Figure 4.6: The three axes of aircraft stability (n.d.)

The payload positioning has minimal impact on yaw control. However, the tank should not be placed far from the yaw axis to avoid undesirable moments from wind gusts. Yaw control is managed by the dihedral angle and V-tail configuration. Similarly, roll control is achieved through aerodynamic surfaces, ensuring the design is symmetrical along the longitudinal centerline, including centering the tank within the bottle-made fuselage.

Pitching Moment Analysis

Tank positioning is crucial for pitching stability as it allows adjustment of the center of gravity (CG). In equilibrium, the sum of all moments and forces must be zero. Variations in the angle of attack (AoA) can cause pitching disturbances that impact longitudinal stability. In our case, a positive AoA relative to airflow is beneficial, ensuring the necessary lift for smooth gliding (Hoekstra, 2023).

For longitudinal static stability, a negative change in the pitching moment should occur with a positive change in AoA (Hoekstra, 2023):

$$\frac{\Delta C_m}{\Delta \alpha} < 0$$

More specifically, this means $C_m(\alpha)$. i.e. the partial derivative of the moment with respect of the angle of attack has to be negative:

$$\frac{dC_m}{d\alpha} < 0 \quad \text{or} \quad C_{m_0} < 0$$

This is visually portrayed at Figure 4.7:

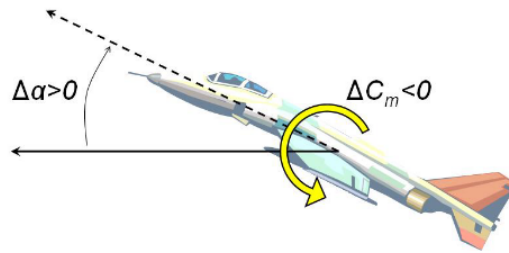


Figure 4.7: Pitching Moment as a result of a positive angle of attack disturbance Hoekstra, 2023

A positive AoA results in upward lift. To counteract this, a negative pitching moment is needed. By performing moment equivalency from the aerodynamic center (where the pitching moment coefficient is constant with AoA), we focus on the moment variation created by the CG due to AoA disturbances. Taking moment equivalency about the aerodynamic center, where lift and drag have no contribution:

$$C_{m_0} = C_{m_a} + (-W) \cdot x$$

With C_{m_0} being the total moment, C_{m_a} the moment about the aerodynamic centre and W the weight acting on the centre of gravity. " x " is the distance between the aerodynamic centre and the centre of gravity, which is in fact the parameter we are interested in, enabling us to find the correct position of the tank. Taking partial derivatives with respect to AoA ($\frac{dC_{m_a}}{d\alpha} = 0$ by definition):

$$\frac{dC_{m_0}}{d\alpha} = (-W) \cdot x$$

As discussed above $\frac{dC_{m_0}}{d\alpha} < 0$ i.e. a clockwise moment for stability. To achieve so, the moment created by weight must also be clockwise and thus negative. The only way to achieve so is to have a positive x and hence, for static stability of a flying wing, the center of gravity must be in front of the aerodynamic center of the vehicle (Hoekstra, 2023).

Neutral Point and Static Margin

Knowing the lift generated by the wings, we can calculate the CG position that ensures stability, called the neutral point. If the CG is behind this point, the aircraft will be unstable; if it's ahead, the aircraft will be stable. The static margin, the distance between the neutral point and the CG, helps us find the optimal tank position. Our goal is to ensure the CG is always in front of the neutral point throughout the flight (Hoekstra, 2023).

5

Detailed Design

To approach the detailed design in the most optimal way possible, the different systems are analyzed separately and only at the end unified to produce the rocket. In this chapter the design of the pressurised water tank, sloshing tank, wing and rear tail will be performed, together with the sloshing tank placement. Additionally, a manufacturing plan is put together and presented together with the bill of materials and the cost breakdown. A risk assessment, is crucial for ensuring safety throughout the manufacturing process and the flight tests and has been included as a separate document.

5.1. Final Configuration

The concept converged to have the following structure. It includes two tanks mounted in parallel with idea to limit the deviations of the centre of gravity throughout the mission, whether the propellant tank is full versus when it is empty. The sloshing tank is mounted beneath the wings enhancing stability at the gliding phase.

Both tanks have approximately the same length, yet differ in design. The propellant tank constitutes of two bottles connected bottom to bottom, to maintain the nozzle-like geometry at the exit. Conversely, the sloshing tank consists of two bottles connected oppositely, replicating an hourglass shape, complemented by other passive anti-sloshing mechanisms.

The space between the tanks houses a wing with a dihedral angle, which will be sized later in the report. A nose cone is added at the front and a V-tail at the end for aerodynamic efficiency. A sketch of the team's concept is provided in Figure 5.1 below:



Figure 5.1: Preliminary Doodle to assist in the visualization of the team's ideation

5.2. Propellant mass estimation

Based on the requirements, the propellant is not to exceed the payload mass currently set at [REDACTED] kilograms. Additionally, the total structure is not to exceed the mass of [REDACTED] at launch. These requirements seriously narrow down our structural mass and propellant mass choices. To optimize, a python script was written (Appendix A). It is based on the thrust to weight formula, the thrust formula and the mass flow formula. Its function can be basically summarized in the following equations:

$$\text{payload_weight} = \text{payload_mass} \times g \quad (5.1)$$

$$\text{structural_weight} = \text{structural_mass} \times g \quad (5.2)$$

$$\text{total_weight} = \text{structural_weight} + \text{payload_weight} \quad (5.3)$$

$$\text{required_thrust} = \text{total_weight} \times \text{thrust_to_weight_ratio} \quad (5.4)$$

$$\text{mass_flow} = \frac{\text{required_thrust}}{v_{\text{exit}}} \quad (\text{the ambient and the exit velocity are considered constant}) \quad (5.5)$$

$$\text{propellant_mass} = \text{mass_flow} \times t_{\text{burn}} \quad (5.6)$$

This is a simplified script giving the following results:

1. The optimal structural mass is [REDACTED]
2. The corresponding propellant mass needed is [REDACTED] to achieve a thrust-to-weight ratio of [REDACTED]
3. The total mass is [REDACTED]

These are the optimal values. Clearly, the total mass is way too close to the limit and the team will try to limit this. However, it's important to try and stay as close to these values as possible. Lastly,

and interesting observation is that propellant mass is the maximum possible as bounded from the regulations, i.e. [REDACTED]

5.3. Pressure vessel design

The main component of the rocket body will be the pressure vessel, it will be manufactured by attaching two water bottles together, each with a volume of 1.5 L. The bottles are made for sparkling water, so the structure is already made to sustain pressure, making them the perfect choice for the pressure vessel. By attaching the bottles together is reasonable to assume a lost of volume [REDACTED] per bottle, resulting in a final volume [REDACTED]. Furthermore, an important parameter to choose is the water fill level, and after an extensive analysis using different online simulating tools (Jackiewicz, n.d.; Heat, n.d.), it was found that 1L of water provides the optimal fill level, aligning with section 5.2 on mass estimation.

Design parameter	Value	Unit
[REDACTED]		

Table 5.1: Design values for the pressure vessel

In order to better visualize the pressure vessel, a 3D render was created and is shown in Figure 5.2:

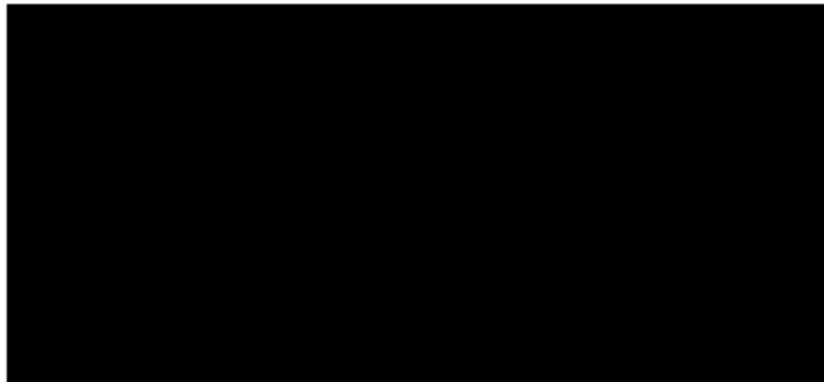


Figure 5.2: Preliminary pressure vessel render

5.4. Wing design

As already mentioned, given that the scoring formula Equation 3.1 mentioned in chapter 3, prioritized horizontal distance travelled and flight time over altitude, the best design option is to build an effective glider. All gliders have a common similarity, a high aspect ratio wing, as it allows to reduce lift-induced drag. For this reason, the maximum wingspan of 2.25m allowed by the regulations will be used (NEUR-DES-02). To optimize lift capabilities, a modified flat-bottom airfoil designed for low speeds is recommended, as it provides the best lift performance at slow speeds.(Johnson, 2005) Using Airfoiltools ("Airfoil Tools", n.d.), the chosen airfoil is a [REDACTED] low Reynolds number airfoil



Figure 5.3: Airfoil

Furthermore a chord length of [REDACTED] is found given the assumed velocity of [REDACTED], the C_l -alpha curve from Airfoiltools, the assumed weight of [REDACTED] a $\frac{L}{W} = [REDACTED]$ and a dihedral angle of [REDACTED] degrees should provide enough roll stability

Design parameter for wing	Symbol	Value	Unit
Span	[REDACTED]	[REDACTED]	[REDACTED]
Chord			
Surface area			
Airfoil			
Dihedral			

Table 5.2: Design values for the wing

5.5. Rear tail

To reduce drag and improve stability a V-tail configuration was chosen, this choice allows for horizontal and vertical stability to be controlled by a single component, ensuring NEUR-FUN-02 is met. The design will first consider a conventional horizontal and vertical tail design, and then combine it into a V-tail configuration.

5.5.1. Horizontal tail

To size the horizontal component a horizontal tail volume coefficient is needed, and from literature (Hall, 2002) a value of V_H [REDACTED] is selected, together with a chord length of c_H [REDACTED], a distance from the center of gravity (assumed to be in the middle of the fuselage during the gliding phase) of $L_H = [REDACTED]$, the surface area and span of the horizontal tail can be computed.

Design parameter for horizontal tail	Symbol	Value	Unit
Span	[REDACTED]	[REDACTED]	[REDACTED]
Chord			
Surface area			
Airfoil			
Volume coefficient			

Table 5.3: Design values for the horizontal tail

Using values from Table 5.2 and Table 5.5, together with the distance of the wing from the center of gravity and the lift curve slope of both the wing and horizontal tail, $\frac{dC_l}{d\alpha}$ and $\frac{dC_{l,h}}{d\alpha}$ respectively, the longitudinal stability can be computed using the theory from Figure 4.4.3.

Design parameter for longitudinal stability	Symbol	Value	Unit
Wing lift curve slope			
Horizontal tail lift curve slope			
Distance wing from CG			

Table 5.4: Design values for the horizontal tail

Then $\Delta C_{L\alpha}$ which is negative as needed

5.5.2. Vertical tail

Due to the absence of active control on the vector, the presence of a vertical tail is only needed for passive stability on the yaw axis. This is achieved by the choice of a $\Delta C_{L\alpha}$ also for this component. This allows the vertical tail to obtain the same dimensions as half of the horizontal tail (one side)

Design parameter for vertical tail	Symbol	Value	Unit
Span			
Chord			
Surface area			
Airfoil			
Volume coefficient			

Table 5.5: Design values for the vertical tail

5.5.3. V-tail sizing

Using (Drela, 2000) it is possible to determine the surface area of one of the two blades of the V shape and the angle with a horizontal plane

$$S_{V-shape} = \frac{1}{2} (S_h + S_v) \quad (5.7)$$

$$\phi = \arctan \left(\sqrt{\frac{S_v}{S_h}} \right) = \quad (5.8)$$

choosing a chord of $c_{V-shape}$, is possible to calculate a span of $b_{V-shape} =$

5.6. Sloshing Tank

The main part of this project is the creation of a successful sloshing tank design. This will be done in two separate parts, one tackling the tank itself, and the other tackling the positioning of the tank.

5.6.1. Tank Design

The design of the tank is the most critical part as the stability of the rocket strongly depends on how sloshing can be mitigated.

The first step is to ensure that the minimum design requirements are met, namely the ones that are provided with the project documentation. Thus, taking into account NEUR-FUN-03 and NEUR-OPER-02, and with the volume of needed propellant estimated to be V_{prop} the volume of water in the sloshing tank is going to be V_{water} as well. To satisfy NEUR-OPER-03, a sloshing tank with a total volume of at least V_{total} is needed. Additionally, it is worth noting that with these design numbers in mind, NEUR-DES-03 can be met since the contents of the tanks form the bulk of the weight of the vehicle.

With the requirements for the contents of the tank out of the way, the focus can be shifted to the shape of the tank and to the means of sloshing mitigation. The two seemingly distinct parts of the design can however be combined to tackle the sloshing problem. Unfortunately, simulation of the sloshing phenomenon is not very straight-forward and requires lots of computing power in order to create accurate results. Nevertheless, knowledge of the linear sloshing theory (Park et al., 2020, Ibrahim, 2005) and an estimation of the forces produced during flight through a simulation (chapter 6), assisted us in choosing the anti-sloshing mechanisms.

There are several methods that one can consider to reduce the sloshing in a tank, as mentioned in chapter 2. The main method of reducing the effect of sloshing is to decrease the surface area of the liquid that is in contact with the air and therefore free to exhibit wave-like behavior. The direct effect of this is that the sloshing liquid will not carry enough momentum when sloshing.

As a result, the main goal of this design is to create a simple tank that minimizes the aforementioned area. The team has come up with an hourglass-like figure, depicted in Figure 5.4 below:

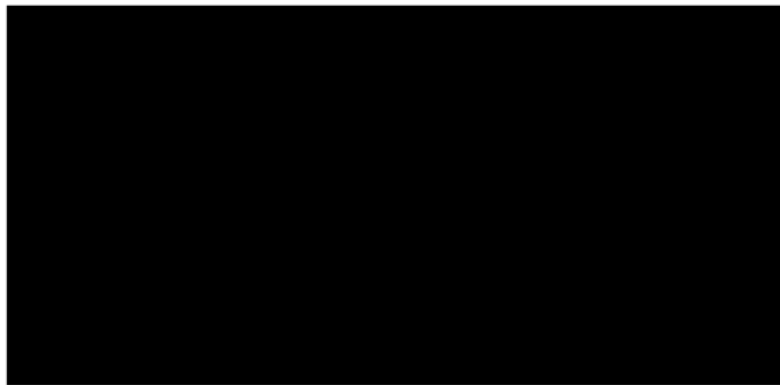
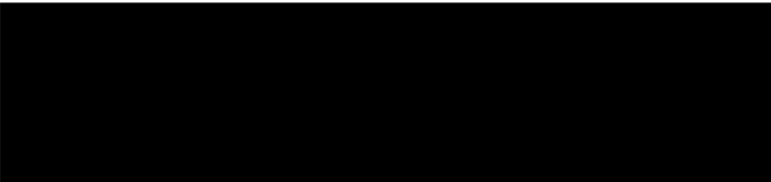


Figure 5.4: Preliminary sloshing tank render

Lastly, to summarize the various features of the sloshing tank, the following list has been created:

- 
-
-
-

5.6.2. Tank positioning

With the preliminary design in mind, it is important to recognize the sloshing will still occur so the placement of the tank will be crucial. Two primary design choices were considered: the placement of the sloshing tank on top of the bottle and the placement of the sloshing tank mounted next to the bottle. To help discern between the two designs, a table containing advantages and disadvantages of the two designs is shown in Table 5.6.

Table 5.6: Advantages and Disadvantages of two sloshing tank placement options

--	--

Due to the shape of the tank and the volume of water that it is going to hold, i was decided to proceed with the second option, namely fitting the tank to the side of the propellant tank. This placement of

the tank will be crucial in getting the required change in flight path and maximizing the distance covered by the rocket.

5.7. Nosecone

A nose cone was added at the front which can be visualized in Figure 5.5 providing aerodynamic efficiency and will be 3D printed. Dimensions are relative to the two bottles connected in parallel and the length is shortened to limit additional mass but provides sufficient surface area to ensure a proper connection with the bottles.

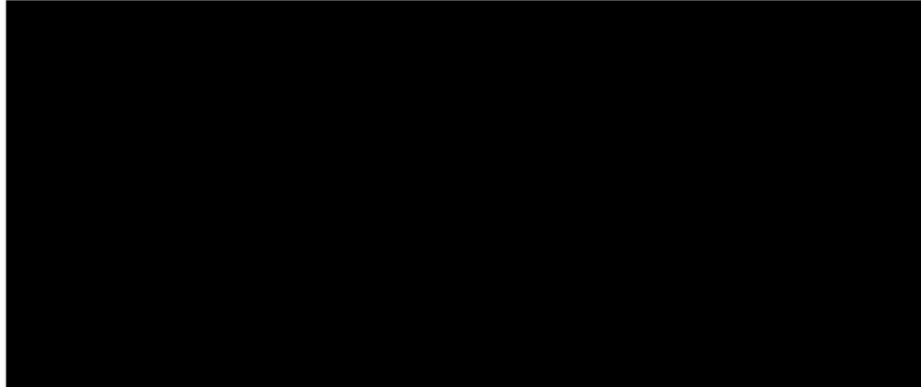


Figure 5.5: Render of nosecone

5.8. Launch Mechanism

The launch mechanism is designed to safely and effectively launch the model. A base, constructed from wooden planks, provides a stable foundation. Four long screws secure the base to the ground, preventing any movement during the pressurization process and ensuring a stable platform for a successful launch. To hold the bottle in place before launch, a U joint is utilized. This U joint is threaded through Chair Corner Joins that are riveted to the supporting planks. The U joint acts as a locking mechanism that keeps the pressurized bottle from launching prematurely.

The model is positioned upright and secured using a cork that has a bike valve inserted through it. This setup ensures an airtight seal. The bike valve is connected to a pump, which will be used to pressurize the bottle with air. Additionally, a rope is attached to the U joint, allowing for a controlled release from a safe distance. At the moment of launch, the operator pulls the rope, which disengages the U joint from the Chair Corner Joins, which result in the bottle to be released, which is then propelled upward by the sudden release of pressurized air escaping from the bottle. The configuration can be seen in Figure 5.6:

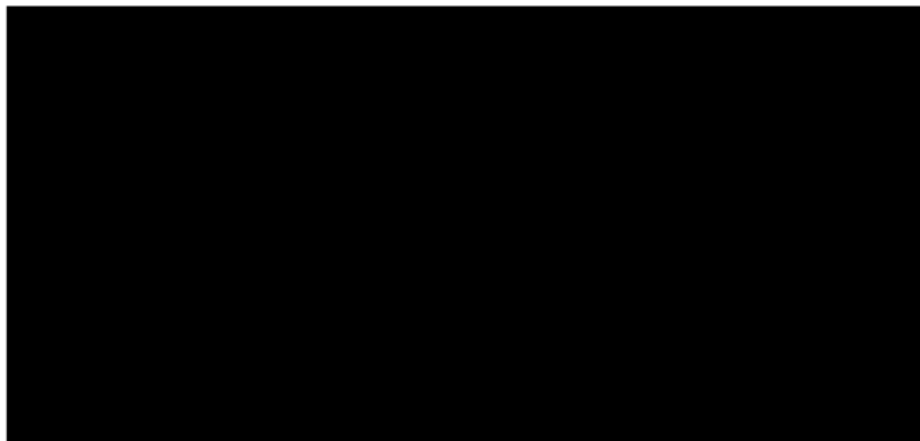


Figure 5.6: Preliminary Doodle of the Launching Pad

Furthermore, the inclusion of a launch tube in this design is highly beneficial, as it allows a restricted nozzle and increases both the altitude and the maximum velocity by limiting mass flow and increasing exit velocity. It is important to size the tube correctly, as it's diameter needs to be close to the nozzle diameter to allow for a faster exit velocity, but not too close as to drastically increase the friction forces. After a iterative process using Jackiewicz, n.d., a launch tube diameter of [redacted] was found to be optimal.

5.9. CAD model

Having completed the design and dimensioning, the following CAD model is produced (Figure 5.7). Minor variations can result during the manufacturing to ensure rigidity of the whole design and the fulfillment of all requirements.



Figure 5.7: Presentation of CAD model

Hereby, the engineering drawing of the model:

[REDACTED]

5.10. Manufacturing Process

For the design to be complete a manufacturing process should be documented highlighting a manufacturing plan and a bill of materials used along with a cost breakdown. These are essential during the competition given the limited time, availability and flexibility, thus necessitating a high level of detail. Along the manufacturing process, attention must be given on the risk assessment, submitted separately, to ensure safety of all members, all people on location and the surrounding environment.

5.10.1. Bill of Materials

To begin with, the Bill of Materials (BOM) is presented. The table below includes the Part Number, Quantity, Title, Description and Cost of the Materials used. An important consideration, is that the costs are rounded up to the nearest integer and sometimes slightly overestimated to account for the worst case scenario and possible price changes between the countries. Materials with a "-" under the cost column are already acquired by a team member and are thus are not included in the total cost consideration.

Part Number	Quantity	Title	Description	Cost (€)

Table 5.7: Bill of Materials

These are the materials and tools required, bringing the total cost in a total of \$[REDACTED], and thus meeting the requirements set in chapter 3 as no Commercial off-the-shelf materials are used and the total cost is less than 500 euros, as stated also in the tables of chapter 6.

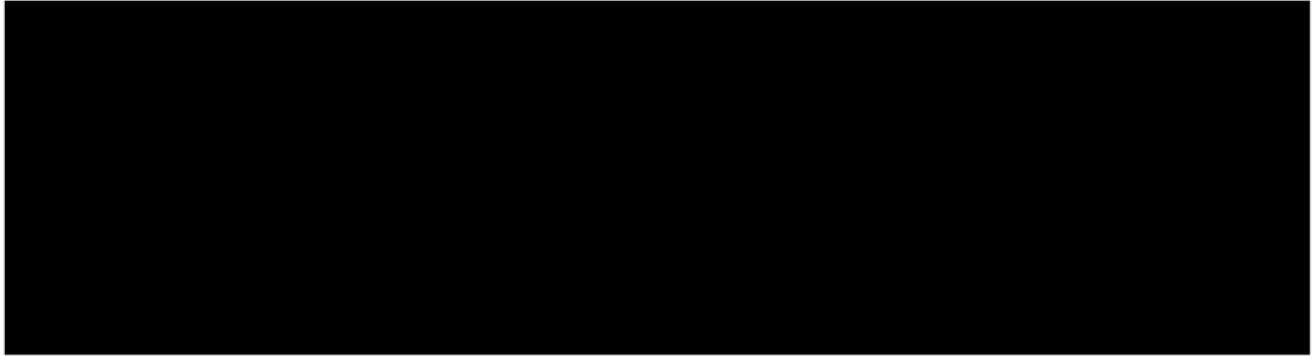
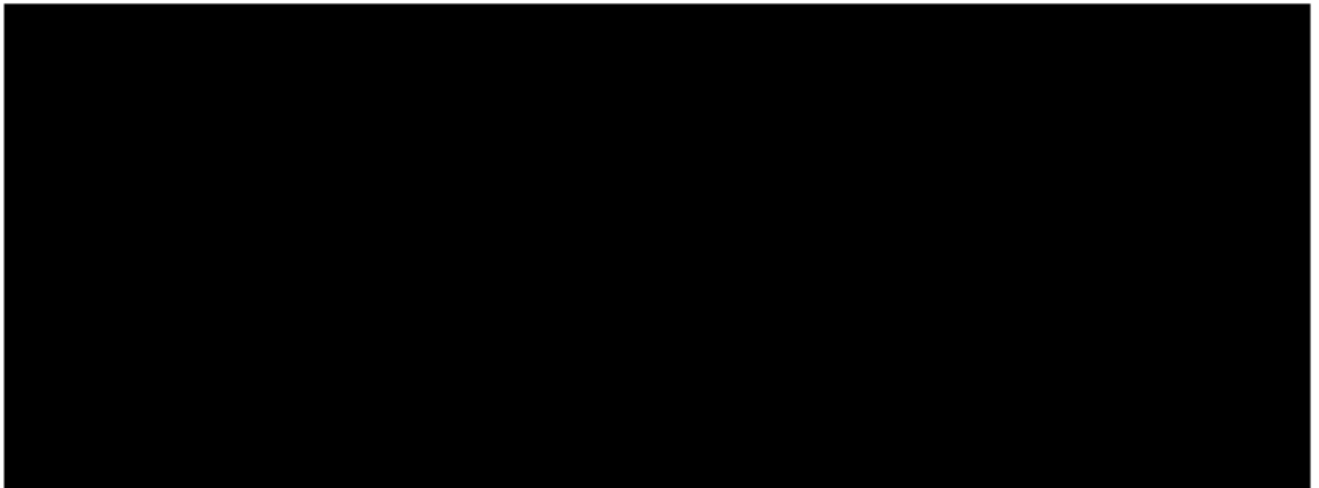
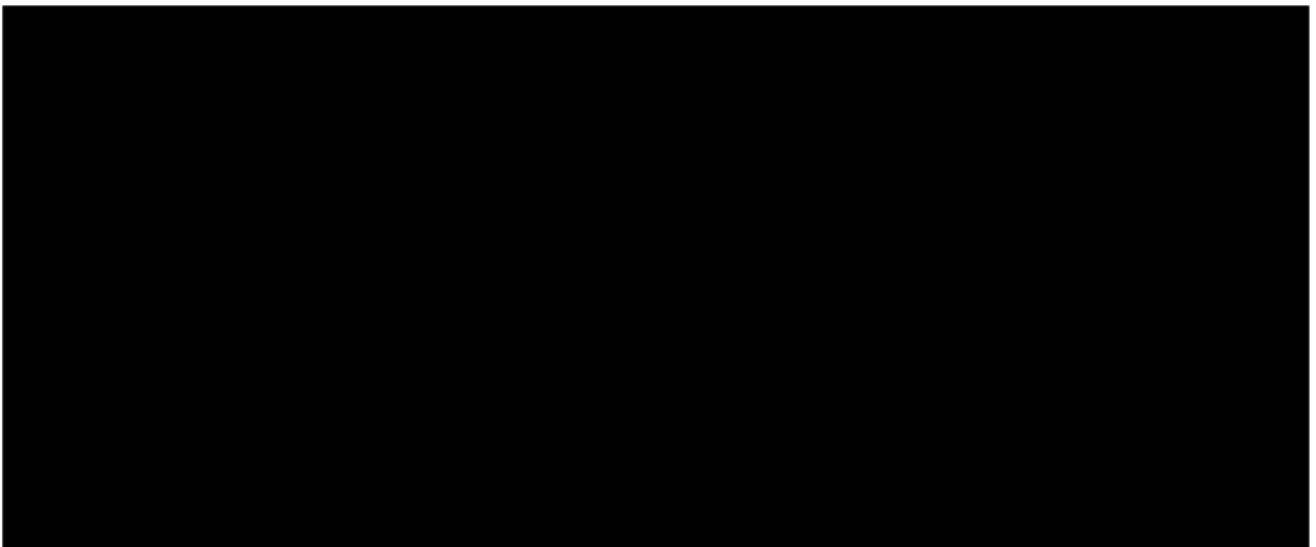
5.10.2. Manufacturing Plan

This subsection is intended to provide crucial information about the manufacturing process of the model. A manufacturing production plan was put together for this purpose with all the essential steps and estimated times for each one. Here, a more extensive procedure and complete plan for the production of the model will be presented in order to demonstrate every single aspect of the manufacturing process. Furthermore, it is considered important to be stated that every sub-step should

be read first before acting. This way, a clear overview is obtained by the manufacturer and irreversible mistakes are avoided. Throughout the manufacturing procedure, the manufacturer should refer to the 3D model, assembly detail drawings and the exploded view to assure the correct placement and dimensions of the parts:

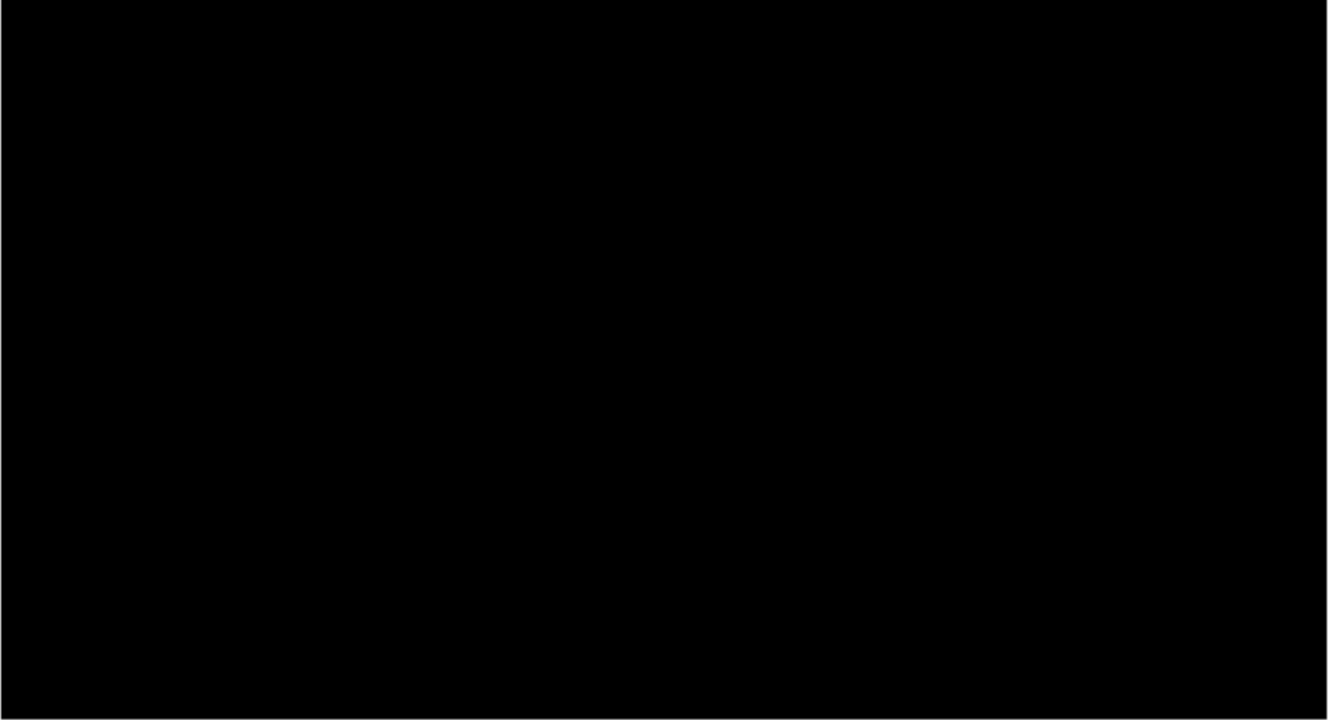
Propellant Tank:

For the propellant tank the procedure developed by Air Command Water Rockets is followed (Surname et al., 2003). Thus the steps will be presented concisely and the team will refer to the website for detailed procedures during manufacturing.

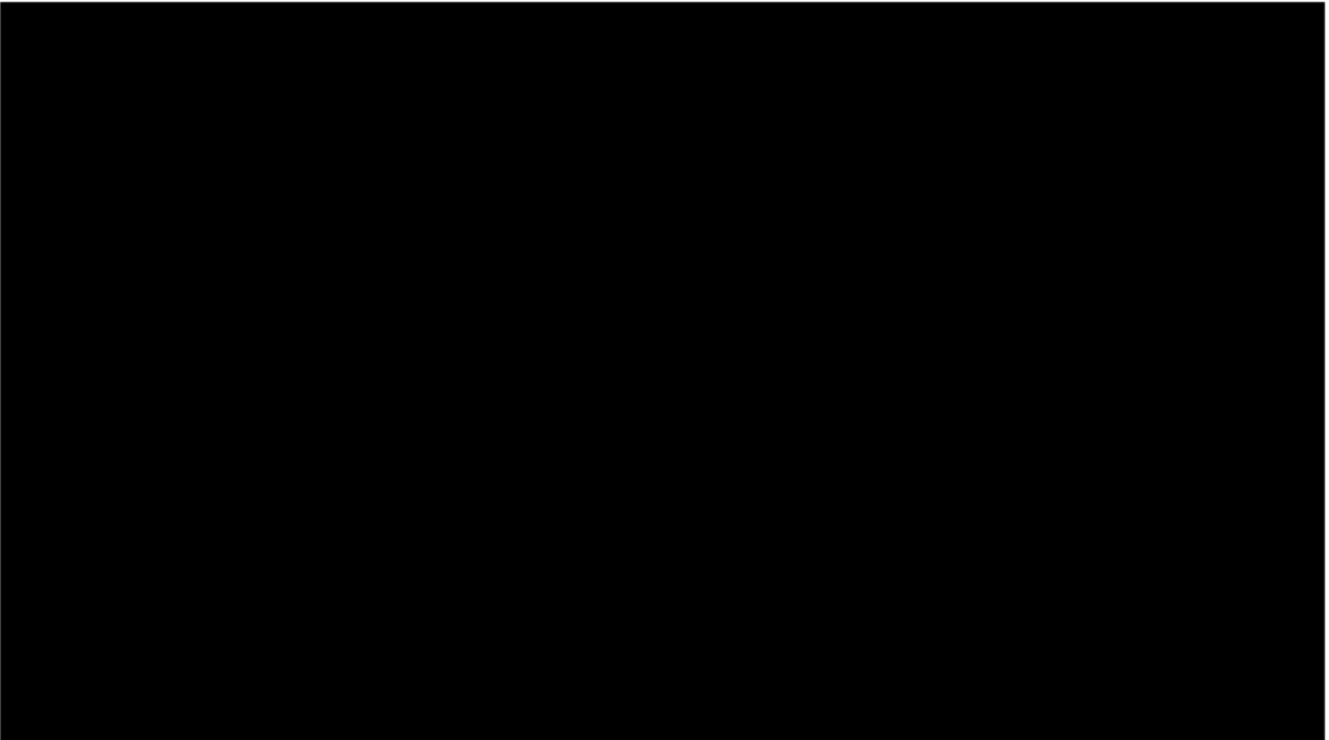
**Sloshing Tank:****Wings:**

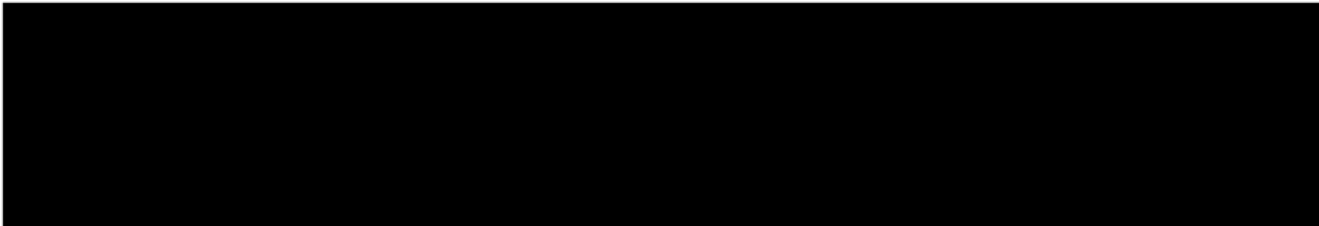


V-tail:

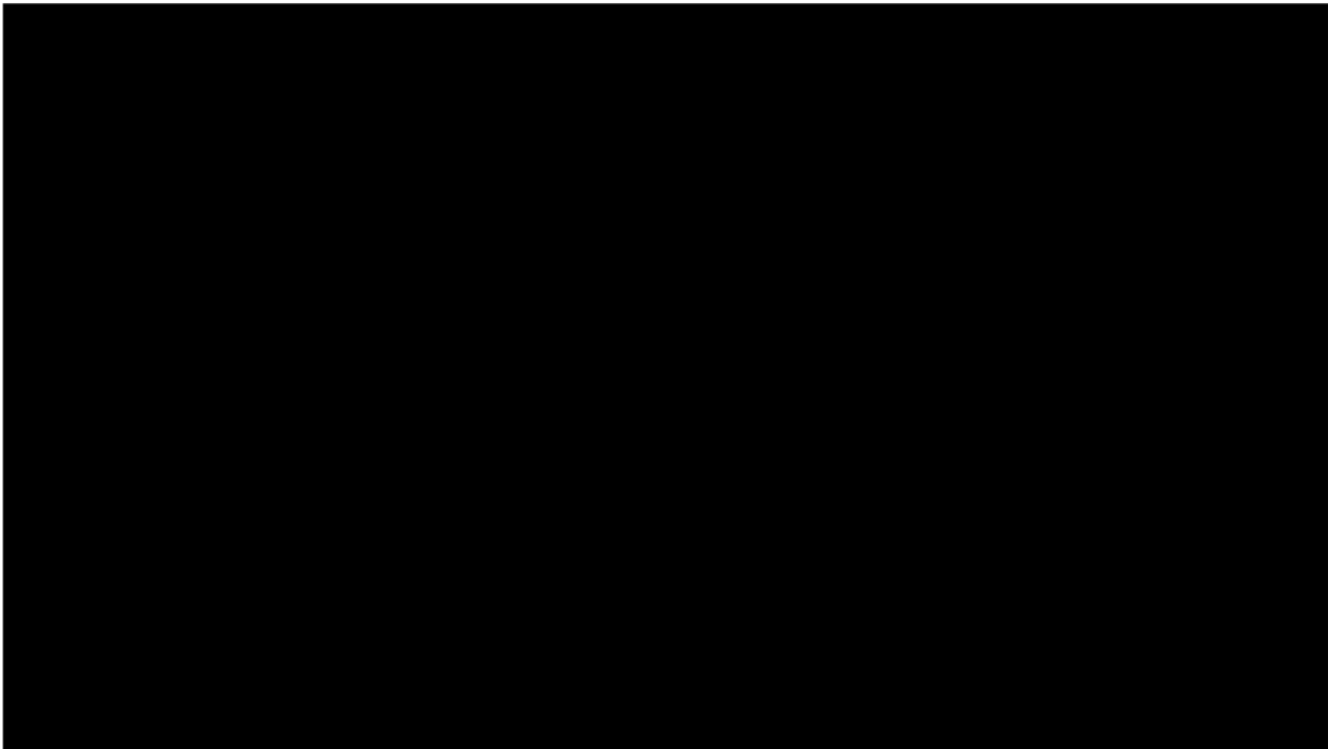


Launch Mechanism:





Assembly Sequence



6

Design Verification and Validation

This chapter explores how the design fulfills the requirements and specification in order to fulfill its purpose, namely an optimised flight profile. Product verification proves that all requirements provided by the competition organisers are met while validation shows that the product accomplishes its intended purpose.

6.1. Simulation Tools Used

To verify the viability of the design and to assess the expected performance, a prototype could be built. However, due to time constraints, a simulation could offer valuable insight into how the rocket is expected to behave. As such, Python code such as the one written on page 33 in Appendix A can be used. The code returns the following estimations for the path of the rocket in Figure 6.1 below.

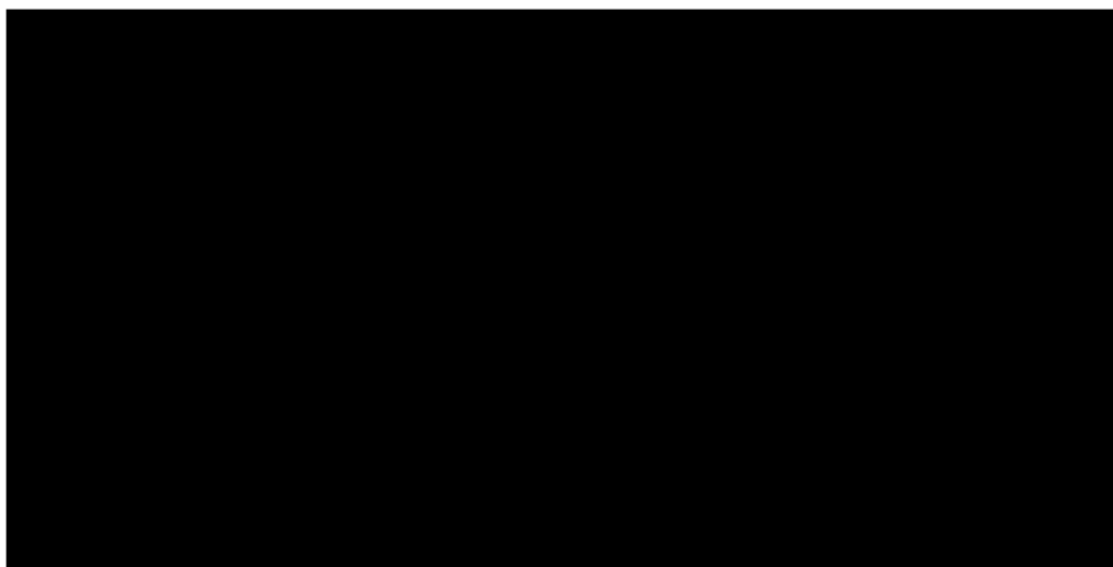


Figure 6.1: The estimated trajectory of a balanced gliding rocket

As it can be seen, the maximum achievable height will be around [REDACTED] and the maximum horizontal distance covered while gliding should be above [REDACTED]. It is worth noting however, that the graph produced above does not take into account the effect of sloshing on the path that the rocket may follow. Instead, this aims to provide an estimate of how high and how far the rocket is likely to go in ideal conditions with the added payload weight.

Finally, the diagram of the forces acting on the rocket during the flight is shown in Figure 6.2 below:

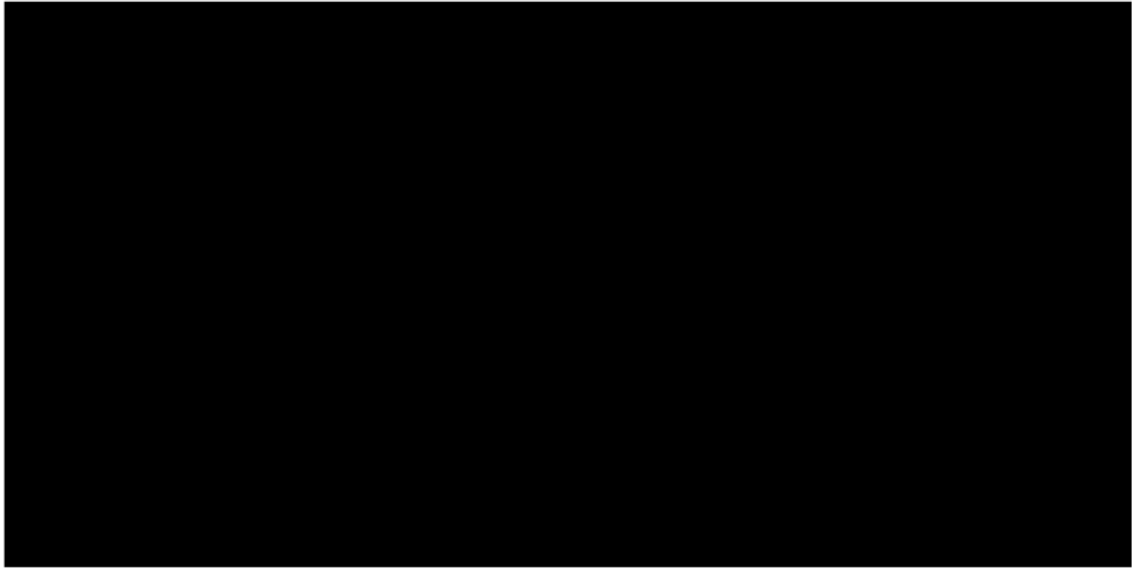


Figure 6.2: The estimated trajectory of a balanced gliding rocket

During the duration of the flight, which is expected to be just above [REDACTED] seconds in ideal conditions, the maximum net force that is going to be experienced should occur right at launch and then it will drop off as the fuel is burned. It is expected that during this stage sloshing will not have a great impact upon stability. However, after the thrust force becomes zero and the only forces acting on the rocket are drag and gravity. the team expects sloshing to start having a negative impact on the stability. Finally, after the apogee is reached at around [REDACTED] gravity, drag and lift start increasing and the net force will slowly begin to increase. It is the change of direction of the gravitational force that will have an impact on the sloshing mass and therefore on the stability of the rocket.

Together with the custom build python code, an online tool was also utilized Jackiewicz, n.d. This tool accepted the design parameters as input and gave altitude, velocity and other outputs. This results can not be taken as fully correct, as the simulation tool can not simulate a non-vertical launch angle, drag and lift generated from the wings and sloshing effects. In the image below

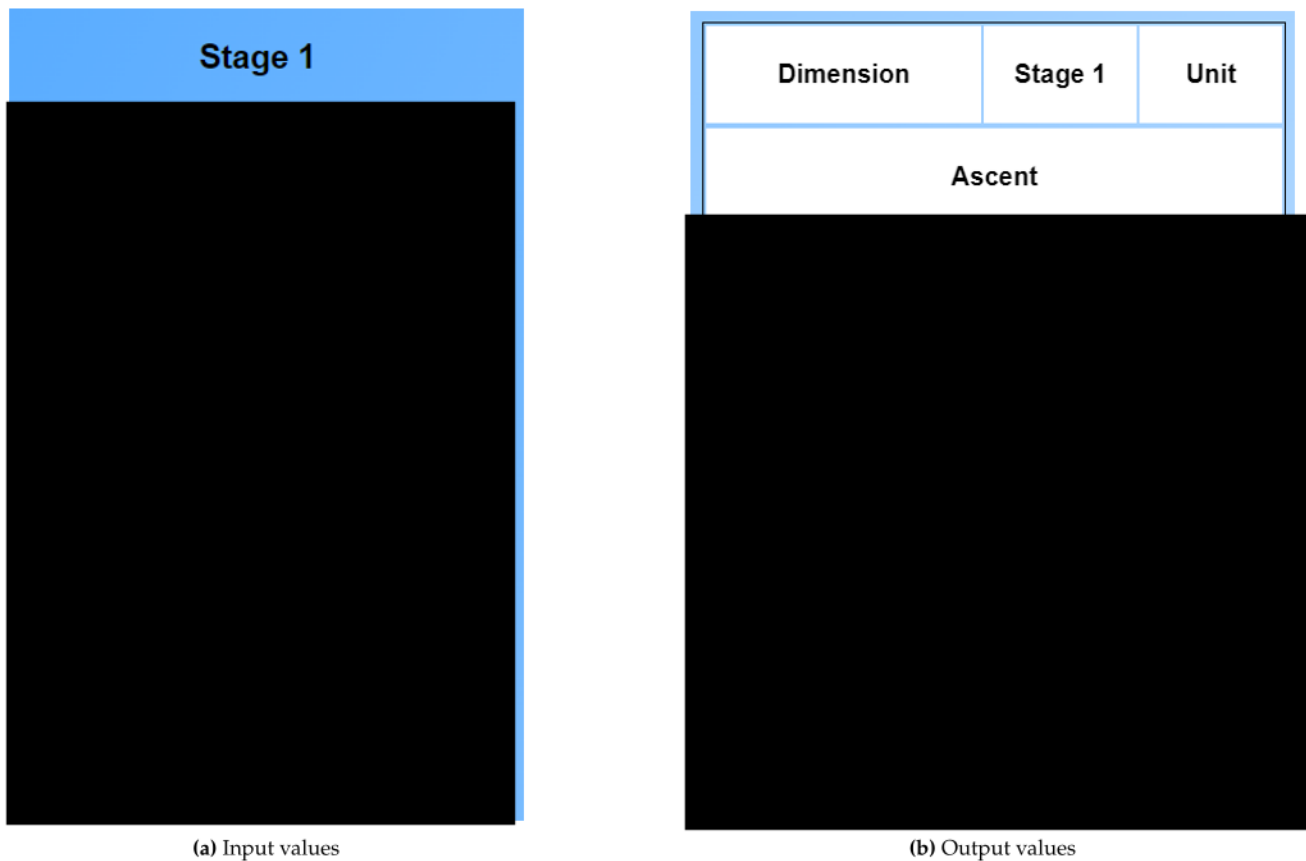


Figure 6.3: Input and output values for the online simulation tool Jackiewicz, n.d.

6.2. Requirements' Assessment

Throughout this report various requirements have been developed, assessed and designed to fulfill them. The team now, proceeds with evaluating the extend on which these requirements have been met. Various ways are being used to achieve that, which include calculations, simulations and numerical practises using Python. The requirement ID, as stated in chapter 3 and an assessment of it is documented in below.

ID	Assessment

Table 6.1: Assessment of Functional Requirements

ID	Assessment

Table 6.2: Assessment of Performance Requirements

ID	Assessment

Table 6.3: Assessment of Design Requirements

ID	Assessment

Table 6.4: Assessment of Operational Requirements

Conclusion

The report's objective was the design of a low-cost, reusable water rocket with a vector and passive stabilization system, addressing the sloshing phenomenon in an additional unpressurized tank. Recognizing the significant challenge of sloshing in aerospace, various mitigation strategies were explored to manage this water displacement effectively.

The final design, approximately 1m in length, satisfied all competition requirements. It was validated by coding and simulation tools and optimised based on materials' availability. The pressurized tank consisted of two bottles connected end-to-end while the unpressurised tank incorporated two bottles connected with a tornado tube in an hourglass shape. Baffles and floating balls were incorporated into the unpressurized tank for sloshing control. A nosecone and a V-tail was used for aerodynamic purposes. Wings were connected between the pressurized and unpressurised tanks at the midway point. The airfoil chosen was the *NACA 0012*. The maximum wingspan of 0.5m was employed and a dihedral angle of 5 degrees was used. The design is presented in Figure 7.1.

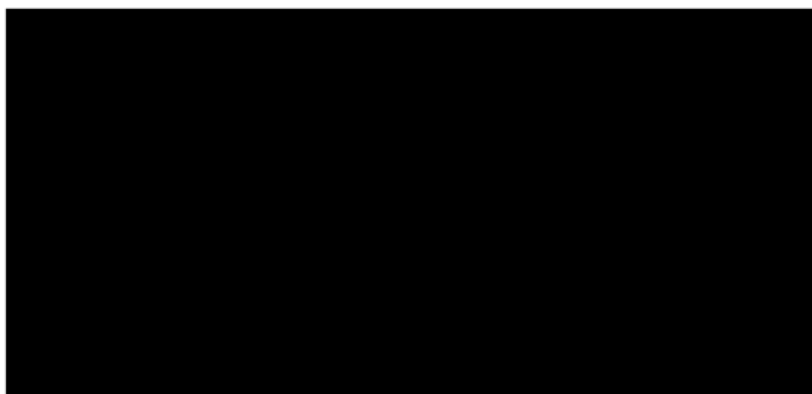


Figure 7.1: Repeated Presentation of CAD model

A manufacturing plan was put together along with the bill of materials and an estimated cost breakdown adding up to a total cost of £100. A risk assessment placed emphasis on ensuring safety in all operations, evaluating the likelihood and the severity of potential hazards.

The presented design, although fulfilling competition requirements, holds potential for further optimisation. A more comprehensive analysis of the sloshing dynamics within the tank was not feasible within the time constraints and identifying our knowledge gap in CFD simulation tools. Future research should focus on a more detailed approach to estimate the forces created during the flight phases and the use of advanced Computational Fluid Dynamics (CFD) tools to predict the motion of the fluid to apply both active and passive anti-sloshing mechanisms.

Bibliography

- Colville, S. (2024). *Sloshing in next generation aircraft fuel tanks*. Retrieved March 8, 2024, from <https://www.ukri.org/blog/sloshing-in-next-generation-aircraft-fuel-tanks/>
- Simonini, A., Dreyer, M., & A. Urbano, e. a. (2024). Cryogenic propellant management in space: Open challenges and perspectives. *npj Microgravity*, <https://doi.org/10.1038/s41526-024-00377-5>(34).
- Ibrahim, R. A. (2005). *Liquid sloshing dynamics: Theory and applications*. Cambridge University Press.
- Behruzi, P., & Rose, F. D. (2018). Active and passive sloshing mitigation in tanks. *International Ocean and Polar Engineering Conference, All Days*, ISOPE-I-18–543.
- Korkmaz, F. (2022). The effect of tank geometry on sloshing forces. <https://doi.org/10.54926/gdt.1192083>
- Hosseini, M., & Farshadmanesh, P. (2011). The effects of multiple vertical baffles on sloshing phenomenon in rectangular tanks. *WIT Transactions on the Built Environment*, 120, 287–298. <https://doi.org/10.2495/ERES110241>
- Utami, S., Trimulyono, A., & Manik, P. (2023). Numerical simulation of the effect of tank shape on sloshing using smoothed particle hydrodynamics. *IOP Conference Series: Earth and Environmental Science*, 1198, 012002. <https://doi.org/10.1088/1755-1315/1198/1/012002>
- Peromingo, C., Sánchez, P., & D. Gligor, e. a. (2023). Sloshing reduction in microgravity with passive baffles: Design, performance, and supplemental thermocapillary control. *Physics of fluids*, 35, 112108. <https://doi.org/10.1063/5.0174635>
- Wang, S., Xu, T.-J., Wang, B., Kanmin, S., Dong, G.-H., & Wang, T. (2023). Numerical simulation of the interaction between nonlinear sloshing flow and side-mounted perforated baffles. *Physics of Fluids*, 35. <https://doi.org/10.1063/5.0158337>
- Dodge, F. T. (1971). *Engineering study of fleible baffles for slosh supression*. National Aeronautics; Space Administration.
- Khouf, L., Benaouicha, M., Seghir, A., & Guillou, S. (2023). Numerical modeling of liquid sloshing in flexible tank with fsi approach. *World Journal of Engineering*, 20, 131–142. <https://doi.org/10.1108/WJE-03-2021-0125>
- Tsao, W., & Huang, Y. (2021). Sloshing force in a rectangular tank with porous media. *Results in Engineering*, 11, 100250. <https://doi.org/https://doi.org/10.1016/j.rineng.2021.100250>
- Gligor, D., Peromingo, C., Salgado Sánchez, P., Porter, J., Fernandez, J., & Mendez, M. (2024). Sloshing mitigation in microgravity with moving baffles. *Acta Astronautica*. <https://doi.org/10.1016/j.actaastro.2024.03.047>
- Gurusamy, S. (2023). Damping of liquid sloshing by floating balls. *Physics of Fluids*, 35. <https://doi.org/10.1063/5.0165870>
- Mushtaq, M. (2023, September). Time of descent formula. <https://www.pw.live/exams/school/time-of-descent-formula/>
- Voskuijl, P. M. (2024). Flight Mechanics. In *AE2230-I Flight and Orbital Mechanics* (Lecture Slides 1 to 3). Delft University of Technology.
- Anderson, J. D. (2011). *Fundamentals of aerodynamics* (6th ed.). McGraw-Hill Education.
- Sutton, G. P., & Biblarz, O. (2017). *Rocket propulsion elements* (4th ed.). John Wiley Sons. (n.d.).
- Hoekstra, P. J. (2023). Pitch Moment Stability. In *Intro to Aerospace Engineering AE1110-I* (Lecture 6: Moments, Control Stability). Delft University of Technology.
- Jackiewicz, W. (n.d.). *Water rocket simulator*. Retrieved May 27, 2024, from <https://waterrocketsimulator.github.io/>

- Heat, C. (n.d.). *Water rocket simulation*. Retrieved May 27, 2024, from <https://cjh.polyplex.org/rockets/simulation/>
- Johnson, P. K. (2005). *About airfoils for flying model aircraft*. Retrieved May 27, 2024, from https://www.airfieldmodels.com/information_source/math_and_science_of_model_aircraft/rc_aircraft_design/plotting_airfoils/about_airfoils.htm#:~:text=If%20the%20plane%20is%20to,cambered%20airfoil%20should%20be%20considered.
- Airfoil tools*. (n.d.). Retrieved May 27, 2024, from <http://www.airfoiltools.com/airfoil/details?airfoil=s7055-il>
- Hall, S. (2002). *How big the tail*. Retrieved May 28, 2024, from <https://www.eaa62.org/technotes/tail.htm>
- Drela, M. (2000). *Quick vtail sizing*. Retrieved May 28, 2024, from <https://charlesriverrc.org/articles/design-and-construction/aircraft-design/tail-design-and-structure/quick-vtail-sizing/>
- Park, W. M., Choi, D. K., Kim, K., Son, S. M., Oh, S. H., Lee, K. H., Kang, H. S., & Choi, C. (2020). Simple analytical method for predicting the sloshing motion in a rectangular pool. *Nuclear Engineering and Technology*, 52(5), 947–955. <https://doi.org/https://doi.org/10.1016/j.net.2019.10.025>
- GAMMA. (2024a). Retrieved May 28, 2024, from https://www.gamma.nl/assortiment/bison-montagekit-super-440-g/p/B483483?store=DELLE&gad_source=1&gclid=CjwKCAjwx-CyBhAqEiwAeOcTdewzHxCgS5786Du-cxm88_PWTweIdAN6ZuvTUiFBLuHLHvtJClMhFxoCepEQAvD_BwE&gclsrc=aw.ds
- GAMMA. (2024b). Retrieved May 28, 2024, from <https://www.gamma.nl/assortiment/tesa-elektrische-isolatietape-15-mm-10-meter-zwart/p/B257781>
- Extrmtextil. (2024). Retrieved May 28, 2024, from <https://www.extremtextil.de/en/mesh-durable-polyamide-106g-sqm.html>
- Etsy. (2024). Retrieved May 28, 2024, from https://www.etsy.com/listing/663420223/white-round-smooth-poly-foam-modelling?ga_order=most_relevant&ga_search_type=all&ga_view_type=gallery&ga_search_query=styrofoam+balls&ref=sc_gallery-1-3&search_preloaded_img=1&plkey=3b78925e07bf648028869b7b7d4c415c8ea7bfbfd%3A663420223&variation0=974173272
- GAMMA. (2024c). Retrieved May 28, 2024, from <https://www.gamma.nl/assortiment/palletplank-vuren-grenen-verouderd-bruin-22x100-mm-200-cm/p/B145115?store=HAALA>
- Rapid. (2024). Retrieved May 28, 2024, from <https://www.rapidtools.nl/en/rapid/rivets-grommets/r5000384>
- Gamma. (2024). Retrieved May 28, 2024, from https://www.gamma.nl/assortiment/stoelhoek-verzinkt-40x40-mm-4-stuks/p/B104733?store=DELLE&gad_source=1&gclid=CjwKCAjwgdayBhBQEIwAXhMxtjFX-x_ydsMrp1sttczvx_4v1GBCidKbeQM0CdZvMDq5S-2-yqWw5BoCPi4QAvD_BwE&gclsrc=aw.ds
- Equipment, S. R. (2024). Retrieved May 28, 2024, from <https://www.summitracing.com/parts/msr-pyubk>
- toolStation. (2024). Retrieved May 28, 2024, from https://www.toolstation.nl/axa-krukstift-rvs-bouten/p37336?channable=002a91696400333733333680%3Fstore%3DBL&gad_source=1&gclid=CjwKCAjwx-CyBhAqEiwAeOcTdcd6ynVbiLYYYkcnbgNB9CDWdw3rB_WBZoxih7DLFjUYsXJZ7-oGBoCR_AQAvD_BwE
- eSUN. (2024). Retrieved May 28, 2024, from <https://esun3dstore.com/collections/3d-filament/products/esun-epla-ss-1-75mm-3d-filament-1kg>
- Wereld.nl, I. (2010). Retrieved May 28, 2024, from <https://www.isolatiwereld.nl/product/eps-isolatieplaat-60se-60mm-1000x1000mm/>
- AMAZON. (2024). Retrieved May 28, 2024, from https://www.amazon.com/WINONS-Wire-Foam-Cutter-WFC0006/dp/B0CHGCRYK24/ref=sr_1_1_sspa?crid=2D8JCPB BKV0VE&dib=eyJ2IjojMSJ9.EM72DOossuffo35spSRd1wFsWmswqfHrkjGSksq5A8I934fu_yg1rQBpBI0xMLWKFoHK2Lo5PnVmCTXCdH3OFKyEKEQ1VOFb6hQhZi1ocwC6kSDQc8NbEEoTYGgyG3mT8Tm2eXa0JDT-lqzv_pBbnxXS5cqqsPlduQPTEJ4UxwBYgS-NamfYPqDUL1vDI_z1FqRfoNfSyXAZSIYtOcOWYonDju8Lk7QEhw91Llap4mnrrwmJfJqzLd-O5S077xa

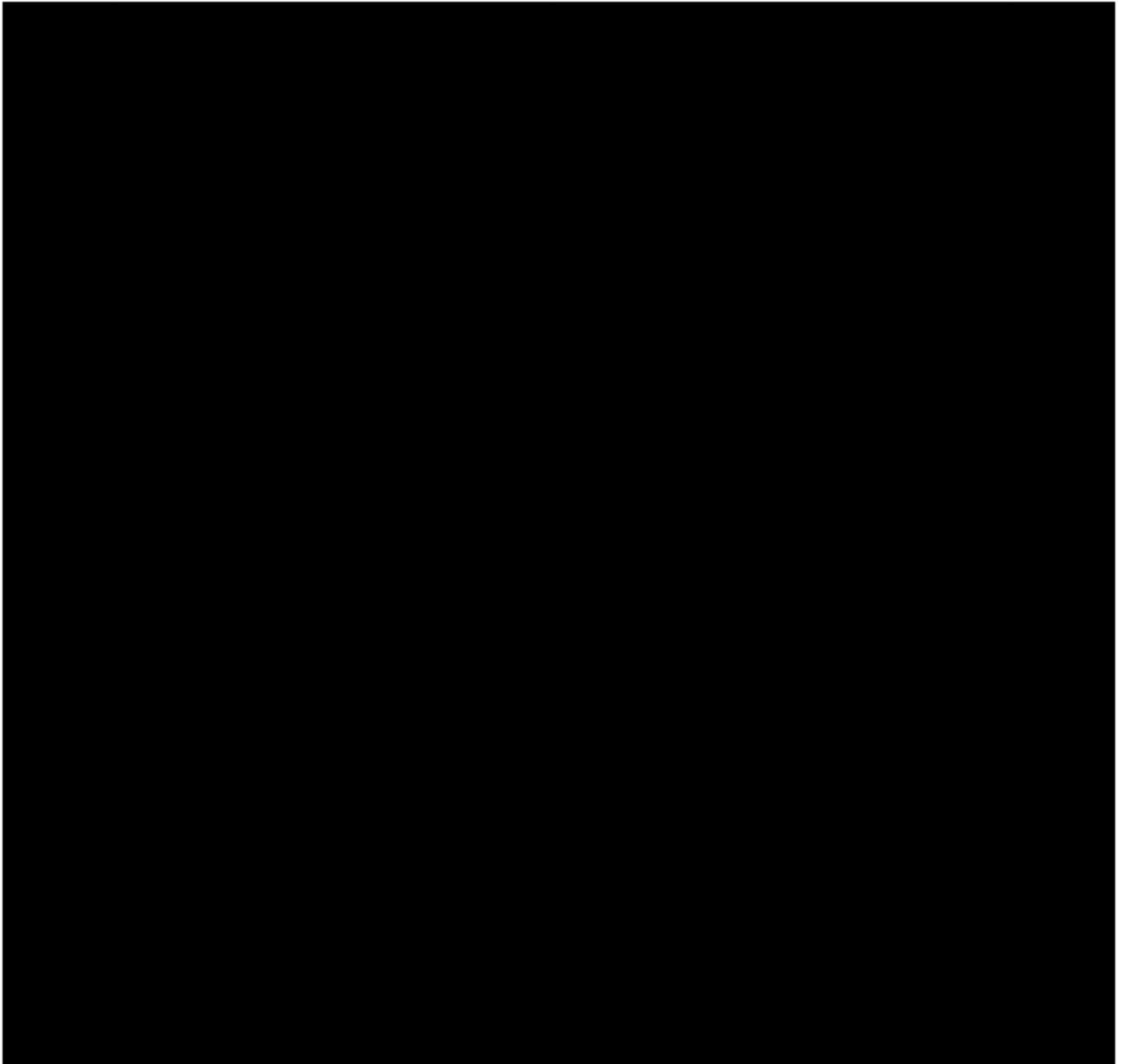
95nMN5zcI8erPL6rP6IlMakhdN1ljDDpvEM3nYbju6_A.KeRyeu5g9pxk9Pptmj51WEJbwSFE
D8AUmGjQt7-qjsU&dib_tag=se&keywords=foam+cutter&qid=1717064150&sprefix=foam+
cutter%2Caps%2C158&sr=8-1-spons&sp_csd=d2lkZ2V0TmFtZT1zcF9hdGY&psc=1

Surname, A. < I., Surname, I., & Surname, I. (2003). *Water rocket construction - advanced tutorials*.
Retrieved October 21, 2023, from http://www.aircommandrockets.com/construction_6.htm

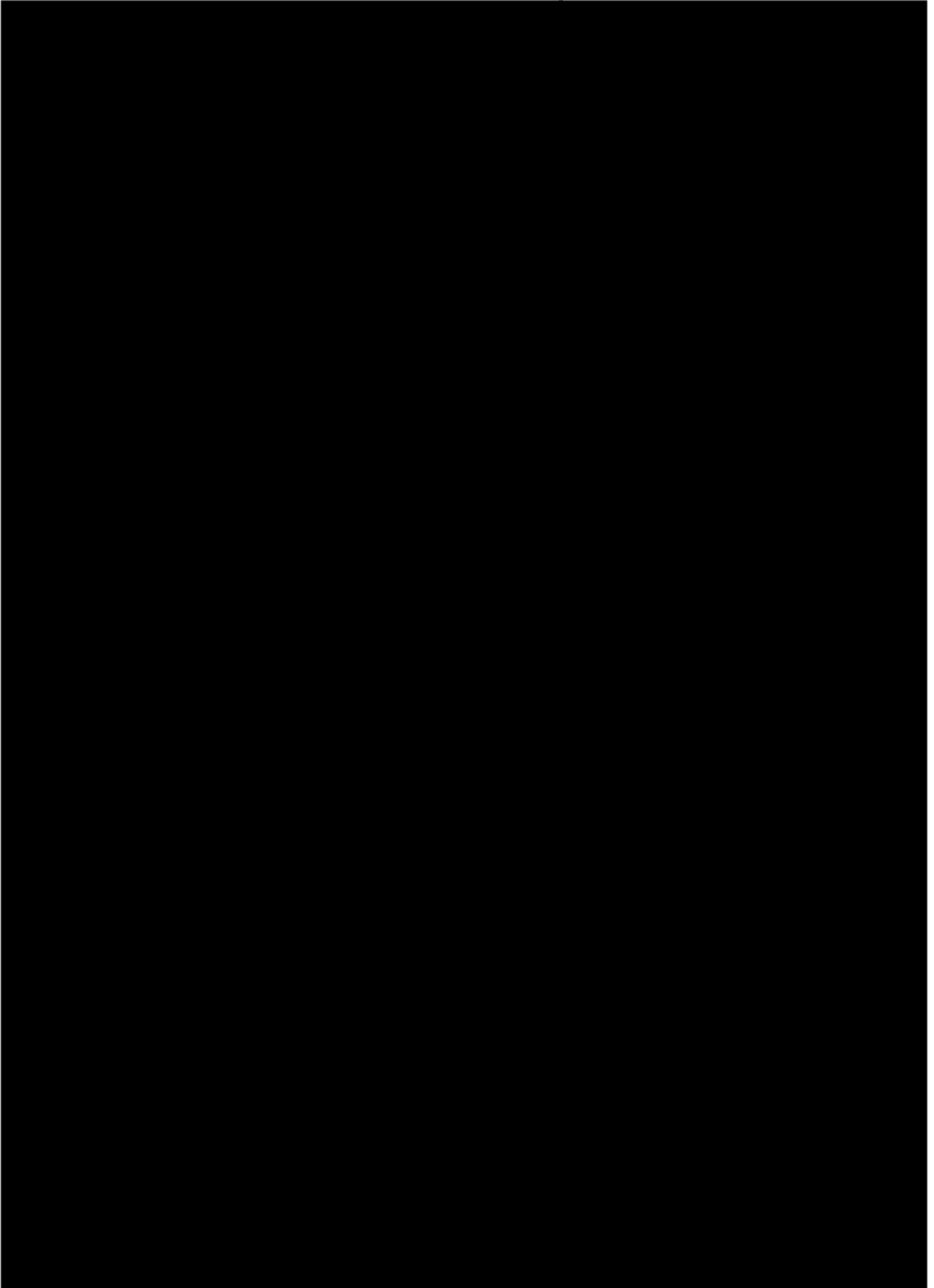


Coding and Simulations

Hereby the code used to calculate the correct payload, structural and propellant mass analogy:



The code that was used to estimate the various forces that may act on the vector is shown below:



100